






Cite this: *Chem. Commun.*, 2023, 59, 14611

Received 1st July 2023,  
Accepted 14th November 2023

DOI: 10.1039/d3cc03182a

rsc.li/chemcomm

## Dendrimersomes: Biomedical applications

Barbara Klajnert-Maculewicz,  \* Anna Janaszewska  and Agata Majecka 

In recent years, dendrimer-based vesicles, known as dendrimersomes, have garnered significant attention as highly promising alternatives to lipid vesicles in a variety of biomedical applications. Dendrimersomes offer several advantages, including relatively straightforward synthesis, non-immunogenic properties, stability in circulation, and minimal size variability. These vesicles are composed of Janus dendrimers, which are polymers characterized by two dendritic wedges with different terminal groups – hydrophilic and hydrophobic. This dendrimer structure enables the self-assembly of dendrimersomes. The purpose of this highlight is to provide an overview of recent advancements achieved through the utilization of biomimetic dendrimersomes in various biomedical applications such as drug and nucleic acid delivery.

### 1. Introduction

The term ‘dendrimersome’ was first coined by Percec and co-workers in 2010.<sup>1</sup> This occurred fifteen years after the publication of two seminal, pioneering papers demonstrating that polystyrene with polypropyleneimine (PPI) dendrimers and polystyrene with polyacrylic acid can form vesicular structures in aqueous phases.<sup>2,3</sup> These structures were observed under transmission electron microscopy. Four years later, the term ‘polymersome’ was used for the first time in another

groundbreaking paper.<sup>4</sup> A polymersome is a vesicle composed of amphiphilic diblock copolymers that self-assemble into a lamellar structure resembling a lipid bilayer. The first reported polymersome was created using polyethyleneoxide–polyethylene, and its membrane was nearly ten times tougher and at least ten times less permeable to water than a phospholipid membrane.

The vast range of copolymer chemical structures has given rise to a frontier of artificial liposome-like vesicles. Fig. 1 illustrates the similarities and differences in structures between liposomes, stealth liposomes, polymersomes, and dendrimersomes. In the case of dendrimersomes, their membrane is built from amphiphilic Janus dendrimers. These dendrimers are composed of two dendritic wedges with different terminal

*University of Lodz, Faculty of Biology and Environmental Protection, Department of General Biophysics, Pomorska 141/143, 90-236 Lodz, Poland.*  
*E-mail: barbara.klajnert@biol.uni.lodz.pl; Tel: +48 42 635 44 29*



**Barbara Klajnert-Maculewicz**

*Her research focuses on studying biological properties of nanosystems, especially dendrimers and polymersomes, and their biomedical applications, primarily as drug carriers in anticancer therapies.*

*Barbara Klajnert-Maculewicz earned her PhD in 2002 from the University of Lodz, Poland and conducted postdoctoral studies at the McMaster University, Ontario, Canada. She is a full professor at the University of Lodz, Poland. From 2015 to 2020, she served as an external scientific member at Leibniz IPF in Dresden, Germany. She has co-authored 2 books and 160 articles, and supervised 7 PhD students. She received the L'Oréal-UNESCO Fellowship for Women in*



**Anna Janaszewska**

*Anna Janaszewska obtained her PhD in biophysics from the University of Lodz in 2003. Since 2020, she has been an associate professor at the Department of General Biophysics at the University of Lodz. Her research centers on the cytotoxicity (in vitro and in vivo) of various dendrimer groups and their applications in medicine, particularly as carriers of anticancer drugs and anti-amyloid agents in neurodegenerative diseases. She continues to investigate different types of polymers as carriers of poorly soluble drugs.*



## Highlight

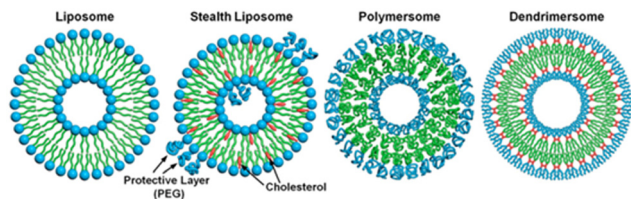


**Fig. 1** A comparison of the structures of a liposome, a stealth liposome, a polymersome, and a dendrimerosome. Reproduced from ref. 55 with permission of Proceedings of the National Academy of Sciences of the United States of America.

groups.<sup>5</sup> Half of the dendrimer has hydrophilic end groups, while the other half has hydrophobic end groups (Fig. 2A). The term Janus dendrimer originates from an ancient Roman god often depicted with two faces looking in opposite directions.

It is worth mentioning at this point, to provide a more comprehensive historical perspective, that the development of dendrimerosome synthesis methods would not have been possible without prior advancements in dendrimer synthesis techniques. Furthermore, it should be noted that the biomedical applications of dendrimerosomes described below (excluding those related to membrane mimicry) have been successfully developed for dendrimers. These highly branched macromolecules with a well-defined and precisely controlled structure, have garnered substantial attention in the field of biomedicine due to their remarkable properties and versatility. As standalone entities, dendrimers have demonstrated a wide array of biomedical applications, ranging from drug delivery and imaging to gene therapy and diagnostics. Their modular design, tunable surface functionality, and the ability to encapsulate various therapeutic agents have made them formidable candidates for addressing challenges in the realm of healthcare.<sup>6</sup> Janus dendrimers are no exception in this regard. Their

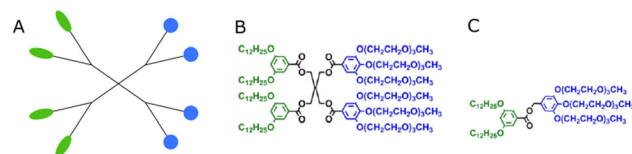


**Fig. 2** The schematic structure of a Janus dendrimer (A) and chemical structures of examples of twin-twin (B) and single-single (C) amphiphilic Janus dendrimers. Reproduced from ref. 8 with permission of American Chemical Society.

biomedical applications are not limited solely to being building blocks for dendrimerosomes.<sup>7</sup>

It should be emphasized that since dendrimers belong to the category of polymers, dendrimerosomes are a specific type of polymersomes characterized by the presence of Janus dendrimers in their membrane.

Dendrimerosomes exhibit relatively uniform sizes, which has been demonstrated through the use of cryo-TEM and dynamic light scattering techniques.<sup>1</sup> The size of the dendrimerosome depends on its chemical composition and the preparation method. Injection of the ethanol solution of dendrimerosomes into water led to vesicles with mean radii ranging from 33 to 732 nm, while hydration experiments with ultrapure water or phosphate buffer saline (PBS) produced giant dendrimerosomes with a diameter between 2 and 50  $\mu\text{m}$ .<sup>1</sup> In the beginning, most amphiphilic Janus dendrimers utilized for dendrimerosome assembly were composed of so-called twin-twin Janus dendrimers (*i.e.*, composed of twin-hydrophobic and twin-hydrophilic dendrons) (Fig. 2B). However, single-single amphiphilic Janus dendrimers (Fig. 2C) were later employed with equal success to build dendrimerosomes, with the advantage of reducing synthetic effort.<sup>8</sup> Additionally, it has been shown that dendrimerosomes with thinner membranes are larger and more stable, and there is a direct correlation between the branching pattern of the hydrophobic part of the Janus dendrimer and the thickness of the membrane. Furthermore, the mass of the vesicle membrane is proportional to the concentration of the Janus dendrimer in water.<sup>9</sup> Predicting the structure and the properties of dendrimerosomes based on the features of the Janus dendrimers is crucial, and many intriguing correlations have already been discovered. For example, it has been demonstrated that the rigidity of dendrimerosomes depends on the melting point or glass transition of Janus dendrimers. Soft dendrimerosomes were obtained when the melting point or glass transition was below room temperature, whereas hard assemblies were characteristic of higher temperature transitions.<sup>8</sup>

The purpose of this review is to focus solely on the therapeutic potential of dendrimerosomes. Our objective is to briefly highlight the primary biomedical fields where dendrimerosomes have been utilized and draw conclusions about their prospects. We do not intend to cover the broad range of synthetic issues related to Janus dendrimers or their self-assembly aspects, which have been comprehensively discussed in an extensive review by Percec and his co-workers.<sup>10</sup> In that review, the authors also introduced a standardized nomenclature for amphiphilic Janus dendrimers and amphiphilic Janus glycodendrimers. Instead,



**Agata Majecka**

*Agata Majecka, a medical biotechnology master's student at the University of Lodz, is currently researching gold-coated liposomes for anticancer therapy. She earned her bachelor's degree at the Lodz University of Technology, International Faculty of Engineering, specializing in molecular biotechnology and technical biochemistry completing an engineering thesis on microorganisms in environmental protection. Her international experience includes a five-month exchange at the University of Camerino and active participation in the Erasmus Student Network. A traineeship at the University of Lodz's Department of General Biophysics fueled her interest in cell culture and drug delivery systems and she was inspired to engage in scientific research.*

*Her international experience includes a five-month exchange at the University of Camerino and active participation in the Erasmus Student Network. A traineeship at the University of Lodz's Department of General Biophysics fueled her interest in cell culture and drug delivery systems and she was inspired to engage in scientific research.*



we have used the nomenclature and abbreviations proposed by the authors, referring to the references to obtain information on specific chemical names and synthesis routes. Although Janus dendrimers can self-assemble into both dendrimersomes and micelles, we have not discussed the medical applications of micelles, which have been extensively studied, especially in the context of drug and nucleic acid delivery. For an overview of these applications, we recommend other reviews.<sup>10,11</sup>

## 2. Drug encapsulation

The potential of dendrimersomes to act as drug carriers was envisioned in the very first article on dendrimersomes.<sup>1</sup> Doxorubicin, an anticancer drug, was loaded into Percec's type of dendrimersomes using the film hydration method. At physiological pH (7.2–7.4), the dendrimersomes were practically impermeable, with negligible drug release. However, under acidic conditions (pH 5.2–5.4) the dendrimersomes released the drug due to cleavage of the aromatic-aliphatic ester groups.

A decade later, Apartsin and his co-workers synthesized a novel category of functional dendritic compounds known as amphiphilic triazine-carbosilane dendrons.<sup>12</sup> These dendrons exhibited self-assembly behavior, forming pH-sensitive dendrimersomes. The researchers proposed that the primary driving force behind the self-assembly process was the interaction between the hydrophobic tails of the amphiphilic dendrons, further stabilized by stacking interactions of triazine moieties. When exposed to an acidic environment, the triazine moieties became protonated, causing disruption of the stacking interactions (Fig. 3). Notably, this pH sensitivity effect was observed at a mildly acidic pH level (below 6.5), which corresponds to the early stages of endosome maturation. As a result, dendrimersomes could release their cargo inside endosomes within cells, creating an efficient drug delivery system. The dendrimersomes effectively encapsulated anticancer drugs, specifically doxorubicin, and methotrexate.

In subsequent studies, the same dendrimersomes were utilized as carriers for rose Bengal (RB), a photosensitizer used in photodynamic therapy (PDT) for skin cancer.<sup>13</sup> The development of new formulations of photosensitizers is necessary to enhance the effectiveness of PDT. By encapsulating RB within dendrimersomes, the cellular uptake of RB, intracellular production of reactive oxygen species, and consequently, the

phototoxicity of this photosensitizer were significantly enhanced.

Another strategy to achieve selectivity is constructing dendrimersomes responsive to light.<sup>14</sup> Such dendrimersomes were formed from the third generation of photodegradable amphiphilic Janus dendrimers. UV light was used to trigger the release of both hydrophilic (fluorescein) and hydrophobic (Nile red) cargo by disintegrating the dendrimersomes. This strategy holds great promise for encapsulation and release applications.

In their study, Laskar and co-workers successfully encapsulated both a hydrophilic dye (R6G) and a lipophilic dye (Nile Red) within dendrimersomes composed of disulfide-linked cholesterol-bearing PEGylated dendrimers. These dendrimersomes demonstrated a redox-responsive behavior, allowing for sustained release of the encapsulated dyes. This release was triggered by higher concentrations of glutathione (GSH), which corresponded to a reducing environment typically found in the intracellular compartment.<sup>15</sup> In a subsequent study, the same research group employed a slightly different approach based on redox responsiveness. They synthesized a PEGylated diamino-butyric (DAB) PPI dendrimer conjugated with the anticancer drug camptothecin using a redox-sensitive disulfide linkage.<sup>16</sup> This dendrimer, upon synthesis, underwent spontaneous self-assembly into cationic vesicles. The remarkable feature of these dendrimersomes was their ability to encapsulate an additional guest molecule, Nile Red, within their nanostructure. This demonstrated their potential to carry multiple encapsulated chemotherapeutic drugs alongside camptothecin. Furthermore, these dendrimersomes exhibited controlled and sustained release of approximately 70% of the conjugated camptothecin in the presence of 50 mM GSH, which mimics the intracellular environment of tumor tissue. Notably, the release occurred gradually, accompanied by breakage of the dendrimersome nanostructures.

The ability to encapsulate lipophilic drugs depends on achieving the right proportion of the size of hydrophilic and hydrophobic dendrons when constructing Janus dendrimers. This was demonstrated by a study on a series of amphiphilic Janus dendrimers derived from two 2,2-bis(hydroxymethyl)propionic acid (bis-MPA) dendritic blocks with differing polarities.<sup>17</sup> The hydrophilic block was made up of a bis-MPA dendron with free terminal hydroxyl groups, while the lipophilic block was functionalized with aliphatic chains derived from stearic acid. Janus dendrimers of varying generations of both dendritic blocks self-assembled into nanospheres. The encapsulation capacity of the amphiphiles was assessed using plitidepsin, a lipophilic anticancer drug. Compounds with higher lipophilic content exhibited better encapsulating ability than those with a larger hydrophilic fraction. The lipophilic component needed to be sufficiently large to provide an appropriate hydrophobic environment for the drug, while the hydrophilic block was necessary to stabilize the system in water.

Propranolol was the next small molecule model drug that was successfully encapsulated during the self-assembly of amphiphilic Janus-dendrimers that were synthesized using

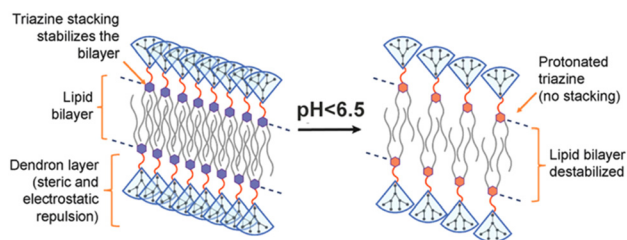


**Fig. 3** A scheme of the pH-dependent behavior of the dendrimersomes' bilayer assembled from amphiphilic triazine-carbosilane dendrons. Reproduced from ref. 12 with permission from the Multidisciplinary Digital Publishing Institute.



## Highlight

click-chemistry by facile coupling of first-generation hydrophobic Percec-type dendrons with two generations of hydrophilic bis-MPA dendrons.<sup>18</sup> Propranolol was mainly encapsulated in the bilayers constituting the dendrimersomes.

In a study by Torre and co-workers, it was observed that multilayer onion-like dendrimersomes exhibited exceptional capability in encapsulating hydrophobic, low-molecular-weight substances.<sup>19</sup> Notably, these dendrimersomes effectively loaded compounds such as a hydrophobic dye called boron-dipyrromethene (BODIPY) and the anticancer drug doxorubicin.

In nanoscience, achieving efficient loading into carriers and precise release of cargo are crucial objectives. However, understanding the process of vesicle breakdown and cargo release is equally significant. One approach to induce the breakdown of dendrimersomes involves incorporating pH-responsive, redox, or light-responsive units into their membrane. Unfortunately, visualizing this process is challenging because electron microscopy, the typical imaging technique for nanometer-scale vesicles, does not allow real-time characterization of vesicle ultrastructure dynamics on the millisecond timescale. To overcome this limitation, the *ortho*-nitrobenzyl group was used as a photolabile unit between the hydrophobic and hydrophilic dendrons of the amphiphilic Janus dendrimers (Fig. 4B).<sup>20</sup> By illuminating the dendrimersomes with a 405 nm laser and employing confocal imaging, it was possible to directly observe the breakdown and subsequent reassembly of the vesicles *in situ*. The experiment involved giant dendrimersomes, and the results demonstrated that, upon illumination for milliseconds to seconds, the dendrimersomes underwent photocleavage, disassembled, and reassembled into smaller vesicles and tubular structures (Fig. 4A). Furthermore, when these dendrimersomes were preloaded with cargo such as the anticancer drug doxorubicin or the small hydrophobic molecule BODIPY, they exhibited significant cargo release. Following a 15 second illumination period, approximately 70–85% of the molecular or macromolecular cargos were released from the dendrimersomes. Importantly, this effect was specific to the photocleavable dendrimersomes, as control dendrimersomes lacking the photocleavable group were unaffected by illumination and did not undergo breakdown or release their cargo.

In Table 1, examples of the use of dendrimersomes as drug carriers are collected, simultaneously presenting the structure

of Janus dendrimers composing the membrane of these dendrimersomes.

### 3. Biomedical imaging and theranostics

Biomedical imaging techniques such as magnetic resonance imaging (MRI) can be improved by the use of gadolinium-based contrast agents. Gadolinium alters the magnetic properties of surrounding water molecules, thereby improving the visibility of certain tissues or abnormalities. In clinical practice, MRI probes based on gadolinium are commonly used for diagnostic purposes.

Filippi and co-workers investigated the potential use of dendrimersomes to carry hydrophilic and/or amphiphilic Gd-complexes as MRI probes.<sup>21</sup> They employed a Janus dendrimer (abbreviated as JD1) based on a pentaerythritol core, consisting of a hydrophobic moiety with two 3,5-bis-dodecyl substituted benzoyl ethers and a hydrophilic segment with one polyester dendritic structure terminating with eight hydroxyl groups. JD1 formed dendrimersomes with a size similar to that of liposomes (approximately 120 nm) and a low polydispersity index. Charged lipids (DMPG or DSPE-PEG200 carboxylate) were incorporated into the membrane to prevent dendrimersome aggregation by electrostatic and/or steric repulsions. Gadoteridol, a clinically approved hydrophilic probe, was chosen, and two methods were used to incorporate amphiphilic agents into the membrane vesicles: (a) JD1 was covalently linked to a Gd-chelate (JD1-GdDOTAMAC<sub>6</sub>), and (b) the lipophilic Gd-DOTAMA(C<sub>18</sub>)<sub>2</sub> complex was included into the bilayer (Fig. 5). Both incorporating strategies proved successful and led to a 3–4-fold increase in relaxivity. Moreover, the enhancement was superior when compared to liposomes with GdDOTAMA(C<sub>18</sub>)<sub>2</sub> incorporated in the lipid bilayer. This improvement can be mainly attributed to the higher water permeability of the bilayer made of Janus dendrimers, which limits the quenching effect on the relaxivity of the paramagnetic units exposed toward the inner core of the vesicles.

In order to simplify the synthesis process, the same group used analogous single-single JD1 dendrimers to create dendrimersomes.<sup>22</sup> Again, Gadoteridol was encapsulated in the inner core of the dendrimersomes. The new dendrimersomes were found to have an equally high water-permeability of the membrane and greater stability compared to the previous twin-twin dendrimersomes. Additionally, the new dendrimersomes showed high biocompatibility and did not have any cytotoxic effects on fibroblasts (NIH/3T3) or murine macrophages (J774A.1 and RAW 264.7). Blood circulation lifetime was also checked by injecting dendrimersomes into healthy BALB/c mice. After the administration, the gadolinium content in mice's blood gradually decreased and was completely eliminated from circulation within 24 hours. Liposomes with Gadoteridol showed a similar trend, but free Gadoteridol was eliminated much more quickly (Fig. 6).

Dendrimersomes based on single-single JD1 dendrimers with a new Gd-chelate called GdDOTAGA(C<sub>18</sub>)<sub>2</sub> incorporated

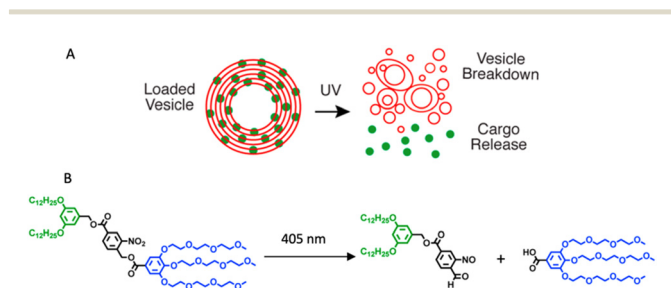
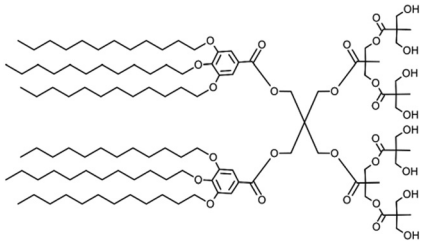
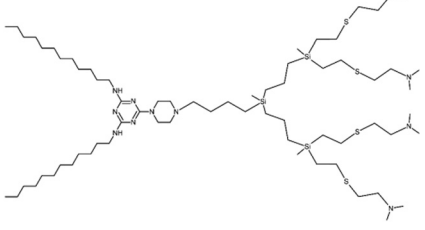
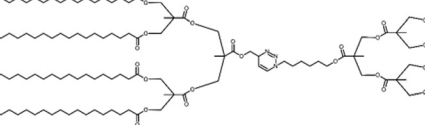
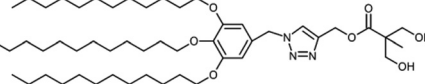
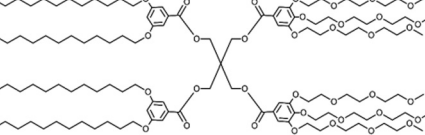


Fig. 4 A schematic showing the photocleavable dendrimersomes breakdown and cargo release upon UV irradiation (A). Photocleavage of amphiphilic Janus dendrimers containing a single *ortho*-nitrobenzyl unit between hydrophobic and hydrophilic dendrons (B). Reproduced from ref. 20 with permission of American Chemical Society.



Table 1 Janus dendrimer structures building dendrimersomes used for drug encapsulation

Dendrimer structure	Drug	Ref.
	Doxorubicin	1
	Doxorubicin Methotrexate Rose Bengal	12 and 13
	Plitidepsin	17
	Propranolol	18
	Doxorubicin	19

into their bilayer were also tested.<sup>23</sup> Liposomes were used as a control nanosystem, and the results were compared to the same nanosystems incorporating GdDOTAMA(C<sub>18</sub>)<sub>2</sub>. Both liposomes and dendrimersomes loaded with GdDOTAGA(C<sub>18</sub>)<sub>2</sub> showed a statistically higher relaxivity compared to the corresponding systems incorporating GdDOTAMA(C<sub>18</sub>)<sub>2</sub>. However, no relevant differences were observed between liposomes and dendrimersomes. The researchers observed no cytotoxicity in cells exposed to dendrimersomes incorporating Gd-DOTAGA(C<sub>18</sub>)<sub>2</sub>. They then investigated the *in vivo* MRI performance of these nanoprobes in an experimental tumor model on a scanner operating at 1 T (40 MHz) and compared the results to analogous dendrimersomes bearing the same percentage of Gd-DOTAMA(C<sub>18</sub>)<sub>2</sub>. Within two hours of injection, both paramagnetic nanovesicles circulated in the blood and caused a general brightening of all the examined organs. However, the imaging and biodistribution profiles suggest that the nanoprobes may have a prolonged *in vivo* retention, which could pose safety concerns for their use in medical applications.

In their subsequent work, the same research group loaded an anticancer drug, prednisolone phosphate (PLP), into dendrimersomes in addition to GdDOTAMA(C<sub>18</sub>)<sub>2</sub>.<sup>24</sup> PLP is approved for the treatment of melanoma, and the researchers

tested this theranostic platform *in vitro* on murine fibroblasts (NIH/3T3), melanoma cells (B16.F10), and human umbilical vein endothelial cells (HUVEC), as well as *in vivo* on a syngeneic murine melanoma model. Liposomes loaded with GdDOTAMA(C<sub>18</sub>)<sub>2</sub> and PLP were used as a comparison. Dendrimersomes were capable of encapsulating PLP with an efficiency and retention ability similar to conventional liposomes. Additionally, the inhibition of tumor growth was slightly more pronounced for dendrimersomes (Fig. 7). The lower cost of dendrimersomes compared to liposomes and their demonstrated effectiveness as an alternative nanovesicle-based delivery system for drugs and imaging agents highlight their potential.

Later Rosati and co-workers introduced a novel series of fluorinated Janus dendrimers that exhibited a flexible and adjustable self-assembly behavior.<sup>25</sup> This discovery has opened up possibilities for the creation of functional dendrimersomes, which hold great potential as <sup>19</sup>F-MRI probes for various biological applications, such as novel theranostic platforms.

An alternative approach to obtaining theranostics involves the use of fluorescent dendrimersomes. These nanoassemblies, combined with their ability to carry drugs, can be utilized for investigating how drugs distribute within a living organism. Fluorescent dendrimersomes can be created by modifying



## Highlight

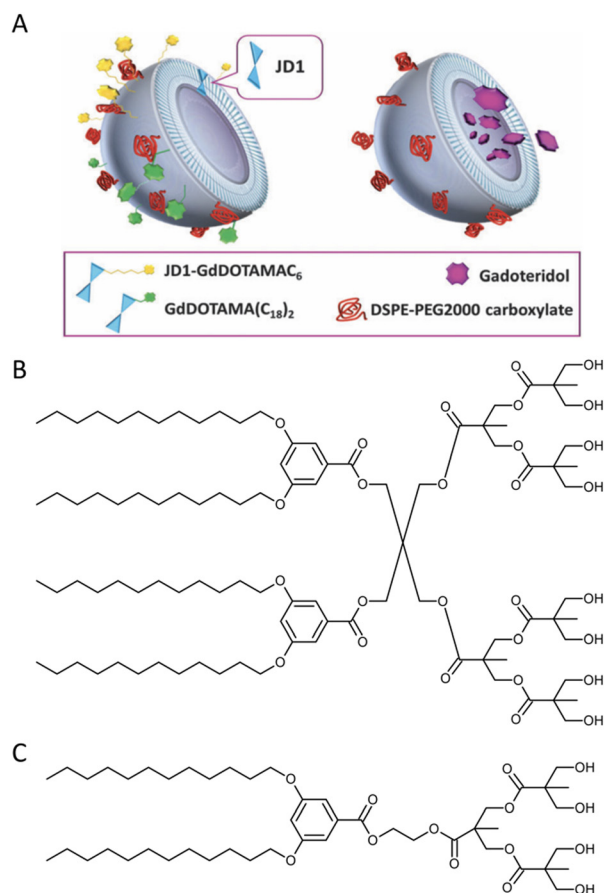


Fig. 5 Dendrimersomes made of JD1 dendrimers incorporating JD1-GdDOTAMAC<sub>6</sub> or Gd-DOATMA(C<sub>18</sub>)<sub>2</sub> into the membrane bilayer (left), and encapsulating Gadoteridol in the inner core (right). Charged lipids (DSPE-PEG200 carboxylate) were incorporated into the membrane to prevent dendrimersome aggregation by electrostatic and/or steric repulsions (A). A chemical structure of twin-twin JD1 dendrimer (B). A chemical structure of single-single JD1 dendrimer (C). Reproduced from ref. 21 with permission of Royal Society of Chemistry.

amphiphilic Janus dendrimers with conventional organic luminogens. However, these materials often suffer from a limitation known as aggregation-caused quenching, which reduces their potential applications. One possible solution to this issue is to use luminogens that exhibit aggregation-induced emission (AIE) properties. These molecules are initially faintly fluorescent when in a dissolved state but become highly luminescent when they aggregate or self-assemble. Bélanger-Bouliga and co-workers successfully developed inherently fluorescent dendrimersomes with AIE properties.<sup>26</sup> These dendrimersomes were obtained by self-assembling amphiphilic Janus dendrimers that were functionalized with tetraphenylethylene (TPE), a commonly used AIE luminogen.

## 4. Nucleic acid delivery

Small interfering RNA (siRNA) shows promise as a therapeutic approach for treating various human diseases. It works by selectively reducing the expression of disease-related genes

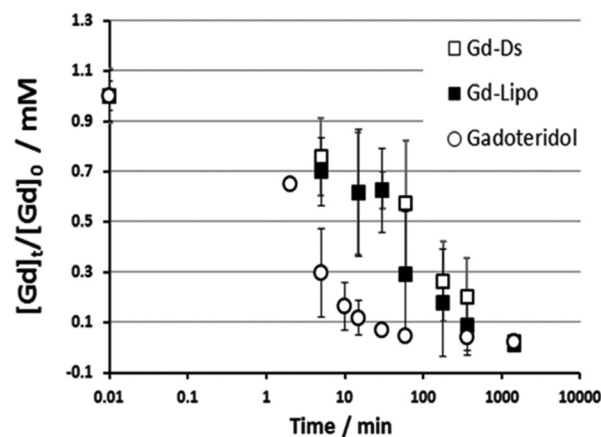


Fig. 6 Kinetics of gadolinium concentration in blood normalized to the injection dose ( $[Gd]_t/[Gd]_0$ ) into healthy BALB/c mice after systemic injection of Gadoteridol, dendrimersomes with Gadoteridol (Gd-DS) and liposomes with Gadoteridol (Gd-Lipo). All animals received equivalent Gadoteridol doses (0.16 mmol per kg bw). Reproduced from ref. 22 with permission of Royal Society of Chemistry.

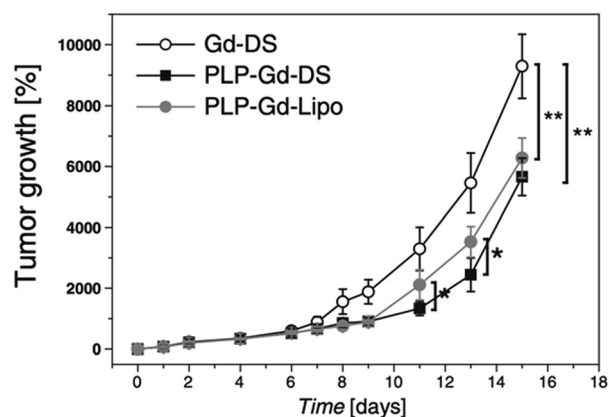


Fig. 7 *In vivo* therapeutic effect measured as tumor growth expressed as the percentage volume increase with respect to the initial tumor volume after systemic administration of paramagnetic dendrimersomes only with imaging agent (GdDOTAMA(C<sub>18</sub>)<sub>2</sub>) (Gd-DS), dendrimersomes with PLP (PLP-Gd-DS) and liposomes with PLP (PLP-Gd-Lipo). Reproduced from ref. 24 with permission of Elsevier.

and inhibiting protein transcription.<sup>27</sup> In theory, siRNA can target and silence any disease-associated genes. However, the success of siRNA therapy greatly relies on effective delivery systems. siRNA molecules are relatively large nucleic acids with polyanionic properties, making them susceptible to rapid enzymatic degradation in the bloodstream, quick elimination by the kidneys, limited penetration through capillary endothelium, and inefficient uptake by cells.<sup>28</sup> Consequently, there is a need to develop delivery systems that offer excellent stability and reproducibility. These systems play a critical role in the clinical application of siRNA-based cancer therapies. To address this challenge, researchers designed and synthesized a cationic amphiphilic Janus dendrimer.<sup>29</sup> The Janus dendrimer featured a cationic hydrophilic head with three amino groups, while its



hydrophobic tail consisted of two fatty chains connected by disulfide bonds (ssJD). As a result, the ssJD could self-assemble into redox-sensitive dendrimersomes known as RSDs. The redox sensitivity of a delivery system plays a crucial role in cancer therapy, given the disparity in GSH concentrations between intracellular and extracellular compartments of living cells. GSH levels are approximately 10 mM intracellularly and less than 10  $\mu$ M extracellularly. Moreover, cancer cells exhibit even higher GSH concentrations, nearly four times greater than those found in normal tissues.<sup>16,30,31</sup> The RSDs exhibited the ability to efficiently bind with siRNA through electrostatic interactions. The formed RSDs/siRNA complexes enabled the effective transportation of siRNA into cancer cells and facilitated the release of siRNA within tumor cells in response to changes in the cellular redox environment (Fig. 8). This targeted release mechanism allowed for specific down-regulation of gene expression. Additionally, RSDs/siRNA complexes demonstrated excellent biocompatibility, ensuring their suitability for clinical applications.

Laskar and co-workers synthesized other RSDs, which consisted of disulfide-linked cholesterol-bearing PEGylated third-generation DAB PPI dendrimers.<sup>15</sup> Two types of dendrimersomes (depending on the cholesterol content) were obtained: low-cholesterol-bearing vesicles and high-cholesterol-bearing

vesicles. The low-cholesterol vesicles efficiently condensed more than 85% of the DNA at all tested ratios, while the high-cholesterol vesicles showed effective condensation at dendrimer:DNA weight ratios of 1:1 and higher. Dendrimersomes assembled from PEGylated DAB PPI dendrimers conjugated with the anticancer drug (camptothecin) were able to form stable complexes with plasmid DNA, condensing more than 85% of the DNA at dendrimer:DNA weight ratios of 5:1 and higher.<sup>16</sup>

These dendriplexes exhibited improved cellular uptake of DNA, up to 1.6 times higher, and enhanced gene transfection, up to 2.4 times higher, in prostate cancer cells compared to the highly effective unmodified DAB dendrimer. The dendrimersomes demonstrated a significant improvement in cellular uptake of DNA. The low-cholesterol vesicles exhibited up to a 15-fold increase in cellular uptake when compared to naked DNA. These vesicles were also capable of enhancing gene transfection in the PC-3 prostate cancer cell line. The most effective transfection was achieved with low-cholesterol vesicle complexes at a dendrimer:DNA weight ratio of 5:1, and high-cholesterol vesicle complexes at a dendrimer:DNA weight ratio of 10:1. These transfection levels were approximately 5-fold higher than those observed with naked DNA. In a subsequent study, the same research group further improved their delivery system by attaching lipidic octadecyl chains to PEGylated DAB PPI dendrimers *via* disulfide linkage.<sup>32</sup> This modification allowed the structural backbone to be cleaved into the corresponding thiols when exposed to a reducing biothiol, such as GSH. As a result, the delivery systems were effectively destroyed, leading to the release of the cargo at the intended site of action. Consequently, the researchers observed an increase in gene expression in prostate PC-3 and DU145 cells when using a dendrimer:DNA weight ratio of 20:1, compared to control unmodified DAB PPI dendrimers.

In mid-2021, a groundbreaking paper was published, presenting dendrimersomes as an alternative mRNA delivery system to lipid nanoparticles (LNPs) for use in COVID-19 vaccines.<sup>33</sup> Despite the unprecedented success of LNPs in Pfizer-BioNTech and Moderna vaccines, the search for novel mRNA carriers remains important. The LNPs used in COVID-19 vaccines consist of four ingredients: ionizable lipids that bind to the mRNA backbone due to their positive charges, PEGylated lipids that help stabilize the particles, phospholipids, and cholesterol to enhance mechanical properties. Although LNPs effectively protect fragile mRNA molecules from degradation by enzymes, they are not without flaws. Firstly, they exhibit stability only at very low temperatures. Additionally, in rare cases, PEG-coated nanoparticles can trigger an anaphylactic reaction. Zhang and co-workers presented a novel mRNA delivery system based on ionizable amphiphilic Janus dendrimer (IAJD) in their study. It involved the development of six libraries containing 54 sequence-defined IAJDs, which were then co-assembled with mRNA into dendrimersome nanoparticles (DNPs) using a straightforward injection in acidic buffers, instead of the complex microfluidic techniques commonly employed for LNPs (Fig. 9).

Remarkably, 81% of the synthesized IAJDs (44 out of 54) exhibited *in vitro* activity, while 57% (31 out of 54) showed

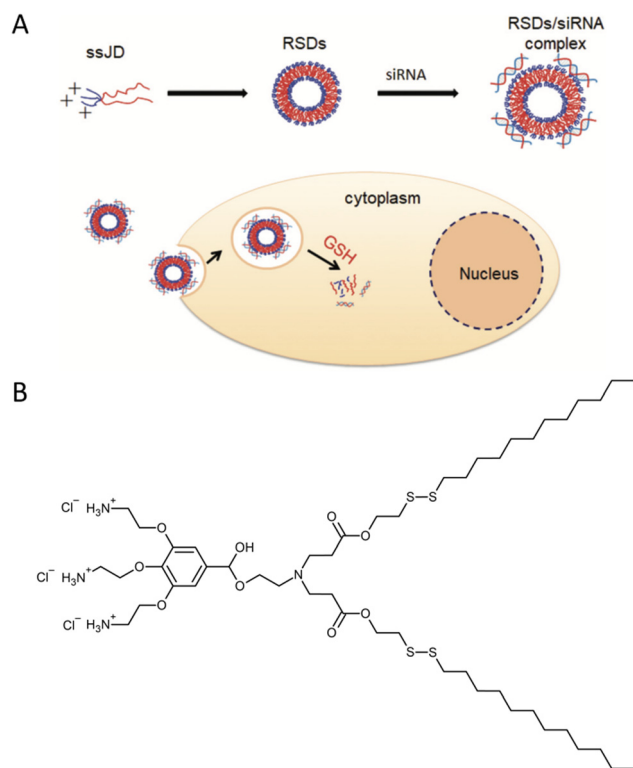


**Fig. 8** A schematic illustration of the cationic redox-sensitive Janus dendrimer (ssJD) that self-assembles into redox-sensitive dendrimersomes (RSDs) to complex with siRNA. The formed RSDs/siRNA was readily internalized into tumor cells, and then rapidly released siRNA upon encountering a high level of glutathione (GSH) to down-regulate the targeted gene (A). The chemical structure of ssJD (B). Reproduced from ref. 29 with permission from the Royal Society of Chemistry.



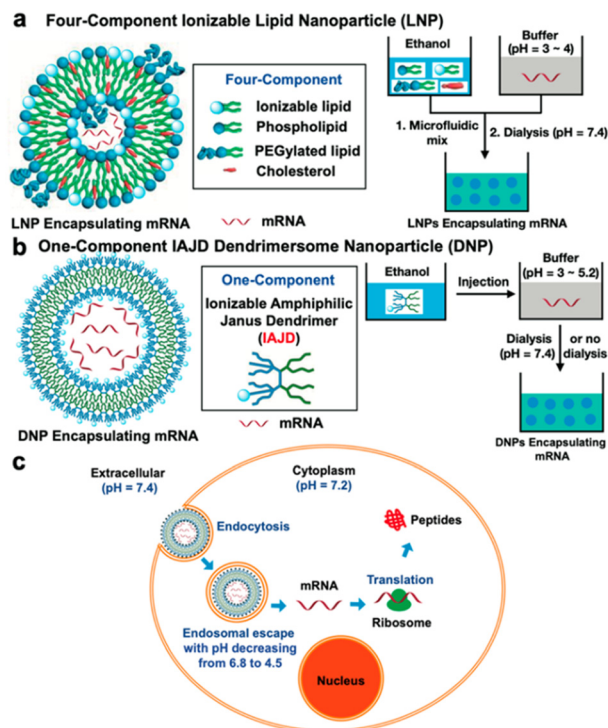


Fig. 9 A schematic illustration of differences in the formation of mRNA complexes with lipid nanoparticles (LNP) (a) and dendrimer nanoparticles (b). Cell-entry and mRNA release from DNP (c). Reproduced from ref. 33 with permission of American Chemical Society.

activity *in vivo*. All these IAJDs remained stable at 5 °C, and some exhibited organ specificity by targeting the lung and achieving higher transfection efficiency compared to the positive control experiments in both *in vitro* and *in vivo* settings. Further studies conducted by the same research team revealed that simple structural modification (*i.e.*, replacement of most of the hydrophilic fragment of the dendron from IAJDs and maintaining only its ionizable amine while changing its interconnecting group to the hydrophobic dendron from amide to ester) resulted in a significant shift in the targeted mRNA delivery.<sup>34</sup> This transformation redirected the delivery from the lung to the liver and spleen. A methodology utilizing screening libraries was employed to discover the essential molecular design principles required for targeted mRNA delivery to organs and the facilitation of activity using a single-component ionizable multifunctional IAJD derived from plant phenolic acids.<sup>35</sup> These IAJDs co-assembled with mRNA, forming monodisperse DNPs with predictable dimensions through the straightforward process of injecting their ethanol solution into a buffer. The strategic placement of functional groups in the 1-component IAJDs demonstrated that hydrophilic regions determined the targeted organs, such as the liver, spleen, lymph nodes, and lungs, while the hydrophobic domain governed their activity.

## 5. Model of biological membrane

The thickness of a giant dendrimer membrane ranges from 5 to 8 nm.<sup>1</sup> It is less than the typical polymersome

membrane, which is usually greater than 8 nm. If the membrane is too thick, it becomes challenging to incorporate pore-forming proteins into it.<sup>36</sup> Dendrimerosomes can provide a significant advantage in this regard. As an example, melittin was successfully incorporated into Percec's type of dendrimerosome.<sup>1</sup> Melittin is a major component of honeybee venom. This natural peptide is known to induce pore formation in membranes therefore it is commonly used to achieve transmembrane leakage.<sup>37</sup> To demonstrate that melittin incorporated in a dendrimerosome increases membrane permeability, the fluorescent dye 1-aminonaphthalene-3,6,6-trisulphonate (ANTS) and its quencher were encapsulated within the vesicle. After the addition of melittin, a dramatic increase in ANTS fluorescence was observed, indicating the release of the dye. This simple experiment proved that dendrimerosomes can serve as a good model of a biological membrane. This concept was further explored by Giustini and co-workers, who successfully solubilized the bacterial reaction centre (RC).<sup>38</sup> RC is an integral membrane protein complex responsible for executing photosynthesis's primary energy conversion reactions.<sup>39</sup> The activity of integral membrane proteins depends on the presence of an organized water-oil-water interface. The (3,5)12G1-PE-BMPA-(OH)<sub>4</sub> dendrimerosome was able to reconstitute the RC from *Rhodospira rubra*, and the RC maintained its photochemical activity. Interestingly, the incorporation of the RC was vectorially orientated with approximately 90% of the protein facing the exterior of the dendrimerosome.

Nitrilotriacetic acid (NTA)-conjugated Janus dendrimers were introduced to functionalize the periphery of the dendrimerosomes to selectively recruit histidine-tagged proteins *via* bioaffinity interactions. Remarkably, this strategy had no detrimental effects on the stability of the dendrimerosomes, while allowing for excellent lateral mobility to support advanced functionalities. One significant advantage of this approach was its versatility, as a large number of recombinant proteins tagged with histidine are available. Consequently, a diverse range of functional proteins and nucleic acids could be utilized to decorate the periphery of dendrimerosomes, enhancing their functional properties without modifying the underlying dendrimerosome platform.<sup>19,40</sup> Li and co-workers designed a strategy for the photorelease of proteins bound to the dendrimerosome surface based on a photocleavage of amphiphilic Janus dendrimers containing a single *ortho*-nitrobenzyl group between hydrophobic and hydrophilic dendrons (Fig. 4B).<sup>20</sup> Upon low doses of 405 nm illumination at short exposure times (<1 s), they observed breakage and rapid release of the outer vesicle layer, thereby liberating the surface-attached protein (Fig. 10).

The aim of creating model membranes is to obtain membranes that mimic cell membranes as closely as possible. An ideal model membrane should replicate the thickness, flexibility, and fluidity of a cell membrane while being resistant to harsh conditions. To achieve this goal, Joseph and co-workers synthesized a Janus dendrimer that consisted of a zwitterionic phosphocholine hydrophilic headgroup attached to a 3,5-didodecyl benzoate hydrophobic dendron (JD<sup>PC</sup>) that assembled





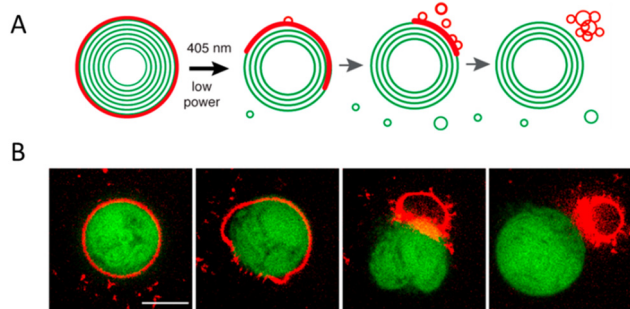


**Fig. 10** A scheme of surface-attached His-tagged protein release from a dendrimerosome exterior (A). Confocal images of the photorelease of His6-RFP protein (red) from a nitrobenzoxadiazole-labeled dendrimerosome (green). Scale bar is 1  $\mu\text{m}$  (B). Reproduced from ref. 20 with permission of American Chemical Society.

into zwitterionic dendrimerosomes (z-DSs) (Fig. 11).<sup>41</sup> They examined how z-DSs could incorporate externally introduced pore-forming peptides. When  $\alpha$ -hemolysin was added to a suspension of calcein-filled z-DS, the fluorescence quickly diminished due to the presence of  $\text{Co}^{2+}$  in the surrounding solution. This observation suggests that a pore was successfully formed allowing  $\text{Co}^{2+}$  ions to enter the vesicle's interior from the external environment. The functional pore was rapidly formed without compromising the integrity of the z-DS. This pore facilitated the transport of ions across a membrane that was otherwise impermeable to  $\text{Co}^{2+}$  (Fig. 12).

The development of artificial cells capable of detecting biomolecules is considered crucial technology for bridging the gap between synthetic and natural cells. To achieve this, the same team created  $\text{H}_2\text{O}_2$ -sensing z-DSs by encapsulating horseradish peroxidase and DNA, and then incubating them with dihydroethidium (DHE), a membrane-permeable compound. Upon the introduction of  $\text{H}_2\text{O}_2$ , horseradish peroxidase catalyzed the oxidation of DHE, leading to the production of

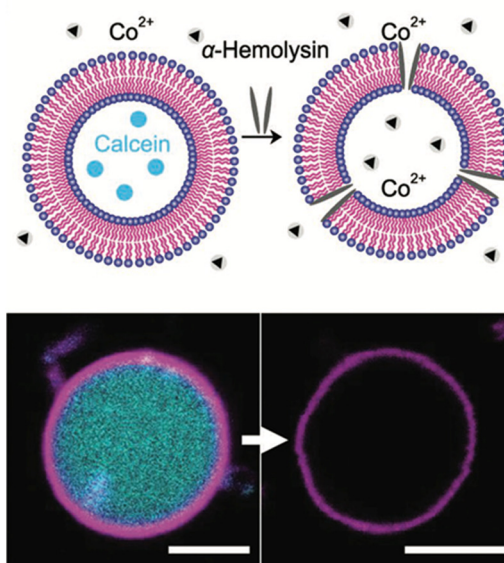


**Fig. 12** A scheme of the pore formation with the addition of  $\alpha$ -hemolysin which enabled the transport and quenching of calcein fluorescence by  $\text{Co}^{2+}$  (top). Confocal laser scanning microscopy images of the addition of  $\alpha$ -hemolysin to calcein-filled z-DSs (bottom). Reproduced from ref. 41 with permission of John Wiley and Sons.

ethidium (E), which intercalated with DNA and produced a red fluorescent product within the interior of the z-DS (Fig. 13). These findings represent significant progress toward the development of synthetic biosensors capable of detecting environments with high concentrations of  $\text{H}_2\text{O}_2$ , particularly in medical applications.

Cell surfaces are often decorated with carbohydrates essential for cellular recognition and communication processes. In order to mimic the ability of biological membranes to recognize sugar-binding proteins, Janus glycodendrimers were designed to self-assemble in water, forming glycodendrimerosomes.<sup>42</sup> One important application of glycodendrimerosomes is in the field of lectin recognition. Lectins are a diverse group of proteins involved in numerous biological processes such as cell-cell recognition, signaling, and adhesion. Glycodendrimerosomes have demonstrated extremely efficient binding to biomedically relevant plant, bacterial, and human lectins, including the plant lectin concanavalin A (Con A), the toxic mistletoe lectin *Viscum album* agglutinin (VAA), the bacterial lectin PA-IL from *Pseudomonas aeruginosa*, as well as the human adhesion/growth-regulatory galectin-3 and galectin-4. It was shown that for glycodendrimers functionalized with glycan, the mode of topological surface presentation and the density of glycan had an impact on vesicle aggregation mediated by multivalent carbohydrate-protein interactions. The covalent connection of the two carbohydrate-binding sites enhanced the cross-linking capacity of homodimeric lectins.<sup>43</sup> Insights into the mechanisms enabling the natural selectivity and specificity of lectins in structural and topological terms can be obtained by mimicking glycan complexity and microdomain occurrence on the surface of glycodendrimerosomes.<sup>44</sup>

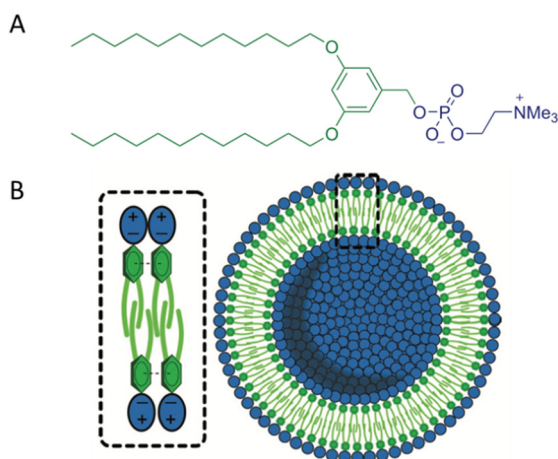


**Fig. 11** The chemical structure of JDPC (A). A scheme of JDPC highlighting the additional cohesive  $\pi$ - $\pi$  interactions between the aromatic rings and interdigitation of the hydrophobic dendrons that drove the assembly into z-DS with improved stability (B). Reproduced from ref. 41 with permission of John Wiley and Sons.



## Highlight

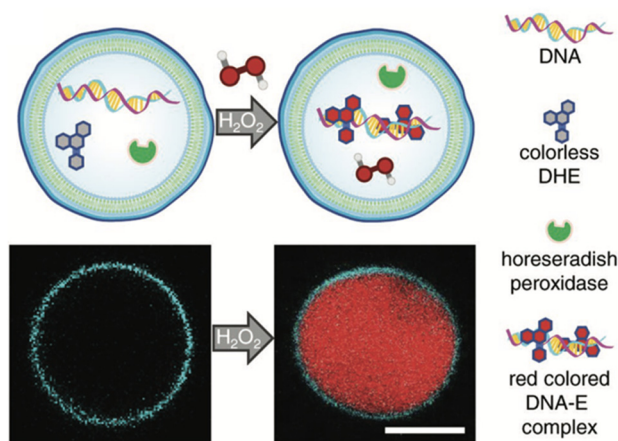


**Fig. 13** A scheme of z-DS with encapsulated DNA, horseradish peroxidase, and dihydroethidium (DHE). Upon the addition of membrane-permeable hydrogen peroxide in the external solution, a red colored DNA-E complex is formed within the vesicle lumen (top). The generation of red fluorescence within the lumen was monitored using confocal laser scanning microscopy. The membrane was labeled with 1 mol% Laurdan. Scale bar: 5  $\mu m$  (bottom). Reproduced from ref. 41 with permission of John Wiley and Sons.

To illustrate the potential of glycodendrimersomes with programmable glycan displays as a model system for revealing the functional impact of natural sequence variations in trans-recognition, the linker length in human galectin-8 was altered, and a single-site mutation (F19Y) was utilized.<sup>45</sup> It was found that lectin capacity as an agglutinin was slightly reduced by the extension of the linker length, and aggregate formation was slowed down at a low ligand surface density. Furthermore, the mutant protein was observed to be considerably less active as an agglutinin and less sensitive to low-level ligand presentation. These results demonstrate the potential of glycodendrimersomes as a model system for understanding the functional impact of natural sequence variations in trans-recognition. The same group extended their investigation by producing Janus glycodendrimers with D-mannose, D-galactose, and D-lactose in the hydrophilic portion.<sup>46</sup> These compounds displayed three distinct topologies, as illustrated in Fig. 14.

Upon injecting THF solutions of the glycodendrimers into water or buffer, all Janus dendrimers underwent self-assembly to form soft unilamellar multivalent glycodendrimersomes. The glycodendrimersomes exhibited specific and potent bioactivity when subjected to agglutination assays with biomedically relevant plant lectin ConA, bacterial lectin PA-IL, and human galectin-7. By conducting agglutination assays using the human lectin Gal-8, the influence of glycans' density, sequence, and topology on glycodendrimersomes bioactivity was revealed.<sup>47</sup> The presentation modes of sugar on the glycodendrimersomes surface resulted in markedly distinct degrees of stable trans-interactions, providing an opportunity to investigate structure-activity correlations. It has significant implications for understanding how glycan display on biological membranes and lectin design work together to achieve their intriguing functions. To investigate the impact of two-dimensional glycan display on

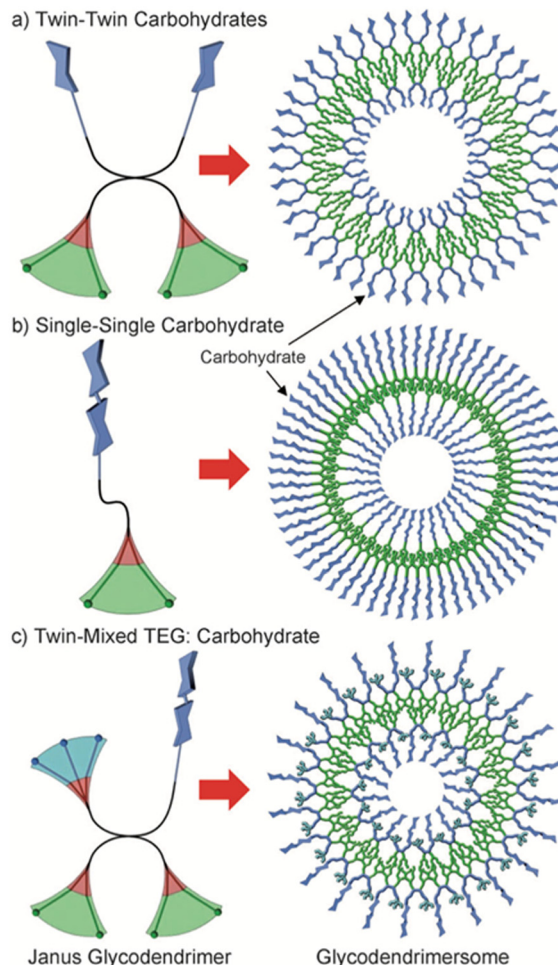


**Fig. 14** Three different topologies of amphiphilic Janus glycodendrimers and the structure of the corresponding multivalent glycodendrimersomes: (a) twin–twin carbohydrates, (b) single–single carbohydrate, and (c) twin-mixed triethylene glycol (TEG): carbohydrate. Color code: hydrophilic blue, hydrophobic green, aromatic red. Reproduced from ref. 46 with permission of John Wiley and Sons.

glycan-lectin recognition, Kostina and co-workers used glycodendrimersomes formed by the self-assembly of sequence-defined mannose-Janus dendrimers.<sup>48</sup> By organizing sugar molecules into nanoarrays, even a simple sugar, like mannose, enhanced recognition by ConA, substantially increasing the kinetic and thermodynamic constant of association.

The similarity in membrane thickness (4.5–4.9 nm) among dendrimersomes, glycodendrimersomes, and lipid bilayers allowed the transfer of intact bacterial membranes from *Escherichia coli* to dendrimersomes and glycodendrimersomes resulting in the formation of cell-like hybrids.<sup>49</sup> The co-assembly process was monitored by enriching bacterial membrane vesicles with a small integral membrane protein MgrB tagged with red fluorescent dye mCherry (Fig. 15).

Hybrid vesicles contained functional porins –  $\beta$ -barrel proteins that enable passive diffusion of small molecules up to 600 Da in size. Membrane permeability was tested by observing the release of an encapsulated yellow-fluorescent dye – rhodamine



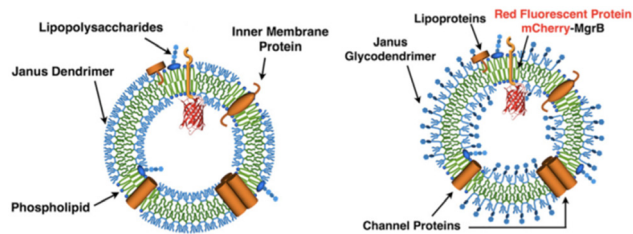


Fig. 15 Hybrid vesicles from *E. coli* bilayer membrane vesicles and dendrimersomes (left) or glycodendrimersomes (right) (reproduced from ref. 49 with permission of Proceedings of the National Academy of Sciences of the United States of America).

6G (Rho) with a size of 479 Da. In contrast, no leakage was observed for a green fluorescent dye calcein with a size of 622 Da. Yadavalli and co-workers made an interesting discovery regarding dendrimersomes' ability to stabilize fragile human cell membranes, leading to the formation of stable hybrid structures combining human membrane vesicles and dendrimersomes.<sup>50</sup> The researchers initially created giant dendrimersomes using carefully selected amphiphilic Janus dendrimers. They then obtained human membrane vesicles through a straightforward centrifugation process of human cells. To co-assemble these components, a dehydration–rehydration technique was employed. As a result, the hybrid vesicles containing both dendrimersomes

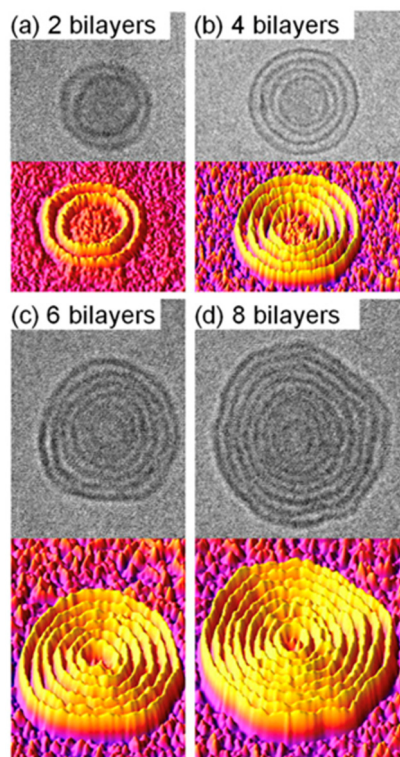


Fig. 16 Cryo-TEM images (upper panels) and 3D surface plots generated by ImageJ (bottom panels) of onion-like dendrimersomes self-assembled from single–single Janus dendrimers in water at concentrations of (a) 0.025 mg mL<sup>-1</sup>, (b) 0.1 mg mL<sup>-1</sup>, (c) 0.2 mg mL<sup>-1</sup>, and (d) 0.5 mg mL<sup>-1</sup>. Reproduced from ref. 55 with permission of Proceedings of the National Academy of Sciences of the United States of America.

and human cell membranes demonstrated bioactivity, as they were capable of binding and aggregating *Escherichia coli* cells using bacterial adhesion protein (YadA). These hybrid platforms hold promise for various applications such as recognition, signaling, and delivery in diverse biological contexts.

Most living organisms contain single-bilayer membranes composed of lipids, glycolipids, cholesterol, transmembrane proteins, and glycoproteins. However, Gram-negative bacteria and the cell nucleus, are unique in that they possess a double-bilayer membrane.<sup>51,52</sup> In addition, more complex membranes can be found in various organelles within cells, such as multivesicular structures of eukaryotic cells and endosomes or multibilayer structures of endoplasmic reticulum.<sup>53,54</sup> This diversity of biological membranes has inspired researchers to create uniform multibilayer onion-like dendrimersomes with predictable sizes and numbers of bilayers. Zhang and co-workers achieved it by injecting a solution of single–single amphiphilic Janus dendrimer into water or buffer.<sup>55</sup> The size and number of bilayers were determined by the concentration of Janus dendrimer, with low concentrations resulting in double-bilayer vesicles and higher concentrations forming multibilayer onion-like vesicles (Fig. 16). Similarly, in the case of Janus glycodendrimers with D-mannose headgroups, the simple injection of a glycodendrimer solution into a buffer resulted in the formation of monodisperse multilamellar onion-like glycodendrimersomes *via* self-assembly.<sup>56</sup> The structural design of Janus glycodendrimers had a notable impact on the resulting glycodendrimersome architecture, including the surface display of D-mannose, which was found to influence the reactivity of the glycodendrimersomes toward lectin.

## 6. Dendrimersomes and bacteria

Dendrimersomes found an interesting application as vesicles capable of engulfing live bacterial cells.<sup>57</sup> The search for synthetic objects capable of endocytosis of living bacteria has been ongoing for some time. This has not been successful with liposomes and polymersomes. Theoretical calculations predicted that it would be possible without the need for active cell machinery if the energy released upon bacterial adhesion to the membrane surpasses the energy required to bend the membrane. To achieve the intended goal, a Janus dendrimer with one dendron characterized by ultra-low adhesion to

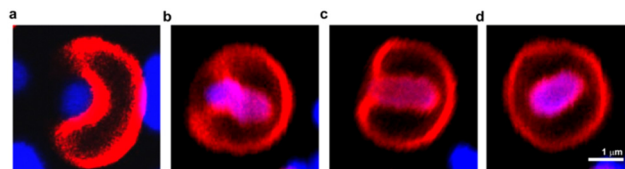


Fig. 17 Confocal laser scanning microscopy images of the process of engulfment of bacteria (blue) by dendrimersome (red). Adhesion of *E. coli* to the DS membrane (a); invagination of *E. coli* into the interior of the dendrimersome (b) and (c); endosome formed with living bacteria inside (d). Reproduced from ref. 57 with permission of American Chemical Society.



bacteria, and the other by high flexibility and high stability was synthesized. This allowed obtaining dendrimersomes capable of endocytosis of *Escherichia coli* in less than one minute after the contact (Fig. 17). The entire process involved the following stages: adhesion, invagination, complete engulfment, and release of an endosome.

The emergence of antibiotic resistance poses a significant global health challenge, necessitating the development of new methods to effectively kill bacteria. Taking inspiration from the localized antimicrobial properties of neutrophil phagosomes, Potter and co-workers created a simple three-component nanoreactor based on dendrimersomes.<sup>58</sup> This nanoreactor exhibited broad-spectrum bactericidal activity. The construction of this nanoreactor involved encapsulating two enzymes, glucose oxidase (GOX) and myeloperoxidase (MPO), within dendrimersomes (referred to as GOX-MPO-DSs). These dendrimersomes were self-assembled from an amphiphilic Janus dendrimer and had a membrane that allowed selective permeability that was permeable for glucose and nonpermeable for encapsulated enzymes. By introducing glucose externally to the GOX-MPO-DSs, the nanoreactor initiated an enzymatic cascade of reactions that resulted in the production of hypochlorite ( $\text{-OCl}$ ), a highly potent antimicrobial agent. This cascade-based nanoreactor demonstrated a powerful bactericidal effect against two important multidrug-resistant pathogens: *Staphylococcus aureus* and *Pseudomonas aeruginosa* (Fig. 18A). It is worth noting that the production of highly reactive species like  $\text{-OCl}$  can be extremely effective in killing bacteria, but it also has the potential to be harmful toward mammalian cells. Therefore, for *in vivo* applications, it is crucial to localize or target the production of these substances to the site of infection in response to a bacterial stimulus. A demonstrated method involved the use of a bacterial toxin as a trigger to locally release sufficient amounts of the substrate (glucose). This was achieved

using lipidic glucose-loaded giant unilamellar vesicles (GLip) (Fig. 18B).

## 7. Conclusions

Nanomedicine is a rapidly evolving field of knowledge. In order to meet the expectations placed upon it, there is a continuous need for the development of new nanocarriers. Among these nanocarriers, vesicles play a significant role. The fact that they are composed of a membrane surrounding an empty core provides unique opportunities for drug delivery. Depending on the hydrophobicity of the drugs, they can reside either in the internal hydrophilic space or within the membrane. Furthermore, vesicles exhibit cell-like properties, and their membrane can successfully mimic a lipid bilayer.

The vast majority of applications described in this article have also been investigated for liposomes and polymersomes. Liposomes are already on the market and have undergone numerous clinical trials.<sup>59,60</sup> Research on the therapeutic applications of polymersomes is ongoing, focusing on the following areas: drug delivery,<sup>61,62</sup> cell mimicking,<sup>63</sup> nucleic acid transport,<sup>64</sup> and antibacterial properties.<sup>65</sup> The translation of polymersomes into clinical settings has not yet been achieved. One of the reasons for this situation is certainly the much later start of research on them compared to liposomes. There are also other objective difficulties for which polymersomes still remain at the preclinical stage, such as achieving biocompatibility comparable to liposomes. Scale-up production of polymersomes is also a significant challenge.<sup>66</sup>

Dendrimersomes, similar to polymersomes, have emerged as an alternative to liposomes. Therefore, it is evident that their presence in the nanoworld, further development of this concept, and exploration of potential applications are justified only if they demonstrate certain advantages over their predecessors. It is known that liposomes derived from natural phospholipids exhibit instability and permeability. Unlike cells, which undergo continuous repair and replenishment processes, liposomes experience degradation processes.<sup>67</sup> Even at low levels of oxidation, this degradation significantly compromises the overall properties of liposomes. Consequently, liposomes demonstrate decreased stability, increased aggregation, fusion, and leakage of encapsulated materials. These characteristics pose significant challenges for the long-term storage and handling of liposomes. On the other hand, polymersomes generally exhibit superior mechanical properties compared to liposomes. They offer enhanced membrane stability due to their higher molecular weight and entangled hydrophobic blocks. However, this increased molecular weight may result in thicker and less flexible membranes, which exhibit limited dynamic behavior.<sup>4</sup> As a result, the integration of natural components such as lipids, peptides, or transmembrane proteins may be difficult, thereby affecting functions that rely on membrane remodeling. Dendrimersomes combine the mechanical strength of polymersomes with the biological functionality of stabilized phospholipid liposomes.<sup>1</sup> They exhibit greater stability at room

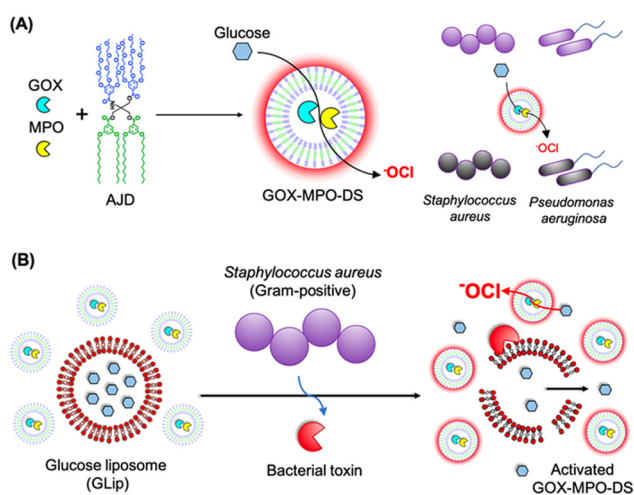


**Fig. 18** Assembly of GOX-MPO-DS from amphiphilic Janus dendrimers (AJD) to obtain an antibacterial nanoreactor capable of killing bacteria (A). Bacterial switch-on mechanism enabled by the toxin-induced release of glucose from giant unilamellar vesicles (GLip) (B). Reproduced from ref. 58 with permission of American Chemical Society.



temperature compared to liposomes made from phospholipids making them less susceptible to degradation, fusion, or leakage over time.<sup>9,41</sup> They also allow for higher loading of hydrophobic molecules into the membrane compared with liposomes.<sup>19</sup> The thickness of dendrimerosome membranes is similar to that of lipid bilayers, making them better mimics of natural cell membranes than most polymersomes.<sup>1</sup> It is worth noting at this point that significant progress has been made in recent years in designing polymersomes free from their original flaws. New strategies for fabricating permeable polymersomes play a particularly important role.<sup>68–70</sup>

The synthetic nature of dendrimers, which form the dendrimerosome membrane, provides flexibility in adjusting molecular morphologies to achieve desired vesicle properties and functions while liposomes have more limited tunability in this regard.<sup>10</sup> A good example is the use of multivalent glycodendrimers with different functionalities (*e.g.*, containing twin–twin and single–single carbohydrates) to obtain glycodendrimerosome membranes that differ from one another.<sup>46</sup> Glycodendrimerosomes represent a promising new category of supramolecular structures with potential applications in nanomedicine. They can serve as mimics of biological membranes with programmable glycan ligand presentations, supramolecular lectin blockers, vaccines, and targeted delivery devices.<sup>43,44</sup> Furthermore, glycodendrimerosomes can be utilized to investigate structure–activity relationships at the multivalent, soft, dynamic, and adaptable surface recognition level, facilitating the exploration of their potential in targeting and lectin blocking.<sup>45,48</sup> The density of glycans on the surface of glycodendrimerosomes plays a pivotal role in their ability to bind to receptors on the target cell. Increasing glycan density can lead to a higher number of contact points with the appropriate receptor, thereby enhancing binding affinity. However, there is also a point at which excessively high glycan density may cause steric hindrance, thereby hindering effective binding to the receptor and consequently decreasing affinity. The ability to test libraries of glycodendrimers with varying surface group densities due to their dendritic structure provided valuable insights into the structure–activity relationship, allowing for the design of glycodendrimerosomes with tailored properties for specific biomedical applications.<sup>45</sup>

Another significant aspect is the biocompatibility of dendrimerosomes, as only nanosystems characterized by low toxicity have a future in clinical research. In this regard, dendrimerosomes show great promise. They demonstrate minimal cytotoxicity, comparable to conventional liposome formulations.<sup>22,23</sup> Furthermore, it is anticipated that many Janus dendrimers incorporating Percec-type dendrons are likely to be harmless, as they may break down into phenolic acids in biological systems, which are known to be nontoxic.<sup>71</sup>

In contrast to polymersomes, research on dendrimerosomes is still in a very early stage. Just compare the number of experimental studies dedicated to polymersomes and dendrimerosomes (770 *versus* 50, according to Scopus). There is a significant lack of in-depth animal studies addressing aspects of toxicity, *in vivo* stability, and biodegradability. The initial reports are promising in this regard, but they are not sufficient.

Furthermore, there is a dearth of systematic comparative studies on dendrimerosomes, both in relation to liposomes and polymersomes. Additionally, similar to many synthetic nanosystems, transitioning from laboratory research to clinical applications requires extensive regulatory compliance and validation.

Among the numerous medical applications of dendrimerosomes presented above, their use as mRNA carriers in COVID-19 vaccines deserves special attention. The achieved lung activity was exceptional for synthetic mRNA delivery and, to the best of our knowledge, one of the highest demonstrated so far.<sup>33</sup> The search for efficient mRNA carriers is not limited to COVID-19 vaccines alone. It is known that this technology also has tremendous potential for cancer treatment. Therefore, dendrimerosomes can play a significant role in this groundbreaking field.

In the case of many nanosystems, including dendrimerosomes, their success will largely depend on the ease of synthesis and cost reduction. Dendrimerosomes belong to self-assembling systems. Therefore, when assessing synthesis ease, the synthesis of the components of this system, namely Janus dendrimers, should be primarily analyzed. Dendrimerosome synthesis can be intricate and time-consuming due to the precise control required over the Janus dendrimer structure. Developing scalable and cost-effective manufacturing processes remains a challenge. However, it is worth mentioning that significant progress has also been made in this area throughout dendrimerosome research. Initially, most amphiphilic Janus dendrimers used for dendrimerosome assembly were composed of twin–twin Janus dendrimers (consisting of twin-hydrophobic and twin-hydrophilic dendrons). However, later on, single–single amphiphilic Janus dendrimers were employed with equal success in constructing dendrimerosomes, offering the advantage of reducing synthetic efforts.<sup>8</sup> However, maintaining the stability of dendrimerosomes during storage and under physiological conditions can be a challenge, similar to potential issues such as aggregation, fusion, or degradation over time, which remain ongoing challenges.

In summary, this research field including both classical polymersomes and their subgroup – dendrimerosomes – holds tremendous potential to revolutionize drug delivery, diagnostics, and various other fields and is worth further exploration. However, addressing the challenges associated with their synthesis, stability, and clinical translation will be essential for realizing this potential.

## Abbreviations

AIE	Aggregation-induced emission
ANTS	1-Aminonaphthalene-3,6,6-trisulphonate
bis-MPA	2,2-Bis(hydroxymethyl) propionic acid
BODIPY	Boron-dipyrromethene
ConA	Concanavalin A
DAB	Diaminobutyric
DHE	Dihydroethidium
DNP	Dendrimerosome nanoparticle



## Highlight

GOX	Glucose oxidase
GSH	Glutathione
IAJD	Ionizable amphiphilic Janus dendrimer
JD	Janus dendrimer
LNP	Lipid nanoparticle
MPO	Myeloperoxidase
MRI	Magnetic resonance imaging
NTA	Nitrilotriacetic acid
PBS	Phosphate buffer saline
PDT	Photodynamic therapy
PLP	Prednisolone phosphate
PPI	Polypropyleneimine
RB	Rose Bengal
RC	Reaction centre (protein complex)
RSD	Redox-sensitive dendrimersome
siRNA	Small interfering RNA
ssJD	Redox-sensitive Janus dendrimer
TPE	Tetraphenylethylene
z-DS	Zwitterionic dendrimersome

## Author contributions

BKM: conceptualization, writing; AJ: visualization, editing; AM: visualization, editing, selecting literature.

## Conflicts of interest

The authors report no conflict of interest.

## References

- V. Percec, D. A. Wilson, P. Leowanawat, C. J. Wilson, A. D. Hughes, M. S. Kaucher, D. A. Hammer, D. H. Levine, A. J. Kim, F. S. Bates, K. P. Davis, T. P. Lodge, M. L. Klein, R. H. DeVane, E. Aqad, B. M. Rosen, A. O. Argintaru, M. J. Sienkowska, K. Rissanen and S. Nummelin, *Science*, 2010, **328**, 1009–1014.
- J. C. M. van Hest, D. A. Delnoye, W. P. L. Baars, M. H. P. van Genderen and E. W. Meijer, *Science*, 1995, **268**, 1592–1595.
- L. Zhang and A. Eisenberg, *Science*, 1995, **268**, 1728–1731.
- B. M. Discher, Y. Y. Won, D. S. Ege, J. C. M. Lee, F. S. Bates, D. E. Discher and D. A. Hammer, *Science*, 1999, **284**, 1143–1146.
- A. M. Caminade, R. Laurent, B. Delavaux-Nicot and J. P. Majoral, *New J. Chem.*, 2012, **36**, 217–226.
- D. A. Tomalia, J. B. Christensen and U. Boas, *Dendrimers, dendrons and dendritic polymers: discovery, applications, and the future*, Cambridge University Press, 2012.
- F. Najafi, M. Salami-Kalajahi and H. Roghani-Mamaqani, *J. Mol. Liq.*, 2022, **347**, 118396.
- S. Zhang, H.-J. Sun, A. D. Hughes, B. Draghici, J. Lejnicks, P. Leowanawat, A. Bertin, L. Otero De Leon, O. V. Kulikov, Y. Chen, D. J. Pochan, P. A. Heiney and V. Percec, *ACS Nano*, 2014, **8**, 1554–1565.
- M. Peterca, V. Percec, P. Leowanawat and A. Bertin, *J. Am. Chem. Soc.*, 2011, **133**, 20507–20520.
- S. E. Sherman, Q. Xiao and V. Percec, *Chem. Rev.*, 2017, **117**, 6538–6631.
- D. R. Sikwal, R. S. Kalthapure and T. Govender, *Eur. J. Pharm. Sci.*, 2017, **97**, 113–134.
- E. Apartsin, N. Knauer, V. Arkhipova, E. Pashkina, A. Aktanova, J. Poletaeva, J. Sánchez-Nieves, F. Javier de la Mata and R. Gómez, *Nanomaterials*, 2020, **10**, 1899.
- K. Sztandera, M. Gorzkiewicz, M. Bałal, V. Arkhipova, N. Knauer, J. Sánchez-Nieves, F. J. de la Mat, R. Gómez, E. Apartsin and B. Klajnert-Maculewicz, *Int. J. Nanomed.*, 2022, **17**, 1139–1154.
- A. Nazemi and E. R. Gillies, *Chem. Commun.*, 2014, **50**, 11122–11125.
- P. Laskar, S. Somani, N. Altwaijry, M. Mullin, D. Bowering, M. Warzecha, P. Keating, R. J. Tate, H. Y. Leung and C. Dufès, *Nanoscale*, 2018, **10**, 22830–22847.
- P. Laskar, S. Somani, S. J. Campbell, M. Mullin, P. Keating, R. J. Tate, C. Irving, H. Y. Leung and C. Dufès, *Nanoscale*, 2019, **11**, 20058–20071.
- E. Fedeli, A. Lancelot, J. L. Serrano, P. Calvo and T. Sierra, *New J. Chem.*, 2015, **39**, 1960–1967.
- S. Nummelin, M. Selin, S. Legrand, J. Ropponen, J. Seitonen, A. Nykänen, J. Koivisto, J. Hirvonen, M. A. Kostianen and L. M. Bimbo, *Nanoscale*, 2017, **9**, 7189–7198.
- P. Torre, Q. Xiao, I. Buzzacchera, S. E. Sherman, K. Rahimi, N. Yu Kostina, C. Rodriguez-Emmenegger, M. Möller, C. J. Wilson, M. L. Klein, M. C. Good and V. Percec, *Proc. Natl. Acad. Sci. U. S. A.*, 2019, **116**, 15378–15385.
- S. Li, B. Xia, B. Javed, W. D. Hasley, A. Melendez-Davila, M. Tingchi Liu, M. Kerzner, S. Agarwal, Q. Xiao, P. Torre, J. G. Bermudez, K. Rahimi, N. Yu Kostina, M. Möller, C. Rodriguez-Emmenegger, M. L. Klein, V. Percec and M. C. Good, *ACS Nano*, 2020, **14**, 7398–7411.
- M. Filippi, J. Martinelli, G. Mulas, M. Ferraretto, E. Teirlinck, M. Botta, L. Tei and E. Terreno, *Chem. Commun.*, 2014, **50**, 3453–3456.
- M. Filippi, D. Patrucco, J. Martinelli, M. Botta, P. Castro-Hartmann, L. Tei and E. Terreno, *Nanoscale*, 2015, **7**, 12943–12954.
- M. Filippi, D. Remotti, M. Botta, E. Terreno and L. Tei, *Chem. Commun.*, 2015, **51**, 17455–17458.
- M. Filippi, V. Catanzaro, D. Patrucco, M. Botta and E. Terreno, *J. Controlled Release*, 2017, **248**, 45–52.
- M. Rosati, A. Acocella, A. Pizzi, G. Turtù, G. Neri, N. Demitri, Nonappa, G. Raffaini, B. Donnio, F. Zerbetto, F. Baldelli Bombelli, G. Cavallo and P. Metrangolo, *Macromolecules*, 2022, **55**, 2486–2496.
- M. Bélanger-Bouliga, B. Andrade-Gagnon, D. T. H. Nguyen and N. Ali, *Chem. Commun.*, 2022, **58**, 803–806.
- S. M. Elbashir, J. Harborth, W. Lendeckel, A. Yalcin, K. Weber and T. Tuschl, *Nature*, 2001, **411**, 494–498.
- D. Castanotto and J. J. Rossi, *Nature*, 2009, **457**, 426–433.
- X.-J. Du, Z.-Y. Wang and Y.-C. Wang, *Biomater. Sci.*, 2018, **6**, 2122–2129.
- M. Huo, J. Yuan, L. Tao and Y. Wei, *Polym. Chem.*, 2014, **5**, 1519–1528.
- P. Laskar, J. Dey and S. Ghosh, *J. Colloid Interface Sci.*, 2017, **501**, 22–33.
- P. Laskar, S. Somani, M. Mullin, R. J. Tate, M. Warzecha, D. Bowering, P. Keating, C. Irving, H. Y. Leung and C. Dufès, *Biomater. Sci.*, 2021, **9**, 1431–1448.
- D. Zhang, E. N. Atochina-Vasserman, D. S. Maurya, N. Huang, Q. Xiao, N. Ona, M. Liu, H. Shah Nawaz, H. Ni, K. Kim, M. M. Billingsley, D. J. Pochan, M. J. Mitchell, D. Weissman and V. Percec, *J. Am. Chem. Soc.*, 2021, **143**, 12315–12327.
- D. Zhang, E. N. Atochina-Vasserman, D. S. Maurya, M. Liu, Q. Xiao, J. Lu, G. Lauri, N. Ona, E. K. Reagan, H. Ni, D. Weissman and V. Percec, *J. Am. Chem. Soc.*, 2021, **143**, 17975–17982.
- J. Lu, E. N. Atochina-Vasserman, D. S. Maurya, M. I. Shalihin, D. Zhang, S. S. Chenna, J. Adamson, M. Liu, H. Ur Rehman Shah, H. Shah, Q. Xiao, B. Queeley, N. A. Ona, E. K. Reagan, H. Ni, D. Sahoo, M. Peterca, D. Weissman and V. Percec, *Pharmaceutics*, 2023, **15**, 1572.
- K. Kita-Tokarczyk and W. Meier, *Chimia*, 2008, **62**, 820.
- M.-T. Lee, T.-L. Sun, W.-C. Hung and H. W. Huang, *Proc. Natl. Acad. Sci. U. S. A.*, 2013, **110**, 14243–14248.
- M. Giustini, C. Bellinazzo, L. Galantini, A. Mallardi, G. Palazzo, S. Sennato, F. Bordini and K. Rissanen, *Colloids Surf., A*, 2012, **413**, 38–43.
- M. R. Gunner, *Curr. Top. Bioenerg.*, 1991, **16**, 319–367.
- Q. Xiao, N. Rivera-Martinez, C. J. Raab, J. G. Bermudez, M. C. Good, M. L. Klein and V. Percec, *Giant*, 2022, **9**, 100089.
- A. Joseph, A. M. Wagner, M. Garay-Sarmiento, M. Aleksanyan, T. Haraszti, D. Söder, V. Georgiev, R. Dimova, V. Percec and C. Rodriguez-Emmenegger, *Adv. Mater.*, 2022, **34**, 2206288.
- V. Percec, P. Leowanawat, H.-J. Sun, O. Kulikov, C. D. Nusbaum, T. M. Tran, A. Bertin, D. A. Wilson, M. Peterca, S. Zhang, N. P. Kamat, K. Vargo, D. Mook, E. D. Johnston, D. A. Hammer,



- D. J. Pochan, Y. Chen, Y. M. Chabre, T. C. Shiao and M. Bergeron-Brelek, *J. Am. Chem. Soc.*, 2013, **135**, 9055–9077.
- 43 S. Zhang, R.-O. Moussodia, C. M. Murzeau, H.-J. Sun, M. L. Klein, S. Vértésy, S. André, R. Roy, H.-J. Gabius and V. Percec, *Angew. Chem., Int. Ed.*, 2015, **54**, 4036–4040.
- 44 Q. Xiao, A.-K. Ludwig, C. Romanò, I. Buzzacchera, S. R. Sherman, M. Vetro, S. Vértésy, H. Kaltner, E. H. Reed, M. Möller, C. J. Wilson, D. A. Hammer, S. Oscarson, M. L. Klein, H.-J. Gabius and V. Percec, *Proc. Natl. Acad. Sci. U. S. A.*, 2018, **115**, 2509–2518.
- 45 S. Zhang, R.-O. Moussodia, S. Vértésy, S. André, M. L. Klein, H.-J. Gabius and V. Percec, *Proc. Natl. Acad. Sci. U. S. A.*, 2015, **112**, 5585–5590.
- 46 S. Zhang, R.-O. Moussodia, H.-J. Sun, P. Leowanawat, A. Muncan, C. D. Nusbaum, K. M. Chelling, P. A. Heiney, M. L. Klein, S. André, R. Roy, H.-J. Gabius and V. Percec, *Angew. Chem.*, 2014, **53**, 10899–10903.
- 47 S. Zhang, Q. Xiao, S. E. Sherman, A. Muncan, A. D. M. Ramos Vicente, Z. Wang, D. A. Hammer, D. Williams, Y. Chen, D. J. Pochan, S. Vértésy, S. André, M. L. Klein, H.-J. Gabius and V. Percec, *J. Am. Chem. Soc.*, 2015, **137**, 13334–13344.
- 48 N. Y. Kostina, D. Söder, T. Haraszti, Q. Xiao, K. Rahimi, B. E. Partridge, M. L. Klein, V. Percec and C. Rodriguez-Emmenegger, *Angew. Chem., Int. Ed.*, 2021, **60**, 8352–8360.
- 49 Q. Xiao, S. S. Yadavalli, S. Zhang, S. R. Sherman, E. Fiorin, L. da Silva, D. A. Wilson, D. A. Hammer, S. André, H.-J. Gabius, M. L. Klein, M. Goulian and V. Percec, *Proc. Natl. Acad. Sci. U. S. A.*, 2016, **113**, 1134–1141.
- 50 S. S. Yadavalli, Q. Xiao, S. E. Sherman, W. D. Hasley, M. L. Klein, M. Goulian and V. Percec, *Proc. Natl. Acad. Sci. U. S. A.*, 2019, **116**, 744–752.
- 51 T. J. Beveridge, *J. Bacteriol.*, 1999, **181**, 4725–4733.
- 52 B. Burke and J. Ellenberg, *Nat. Rev. Mol. Cell Biol.*, 2002, **3**, 487–497.
- 53 I. Mellman, *Annu. Rev. Cell Dev. Biol.*, 1996, **12**, 575–625.
- 54 A. B. Novikoff, *Proc. Natl. Acad. Sci. U. S. A.*, 1976, **73**, 2781–2787.
- 55 S. Zhang, H.-J. Sun, A. D. Hughes, R.-O. Moussodia, A. Bertin, Y. Chen, D. J. Pochan, P. A. Heiney, M. L. Klein and V. Percec, *Proc. Natl. Acad. Sci. U. S. A.*, 2014, **111**, 9058–9063.
- 56 Q. Xiao, S. Zhang, Z. Wang, S. E. Sherman, R.-O. Moussodia, M. Peterca, A. Muncan, D. R. Williams, D. A. Hammer, S. Vértésy, S. André, H.-J. Gabius, M. L. Klein and V. Percec, *Proc. Natl. Acad. Sci. U. S. A.*, 2016, **113**, 1162–1167.
- 57 N. Yu Kostina, K. Rahimi, Q. Xiao, T. Haraszti, S. Dedisch, J. P. Spatz, U. Schwaneberg, M. L. Klein, V. Percec, M. Möller and C. Rodriguez-Emmenegger, *Nano Lett.*, 2019, **19**, 5732–5738.
- 58 M. Potter, A. Najer, A. Klöckner, S. Zhang, M. N. Holme, V. Nele, J. Che, L. Massi, J. Penders, C. Saunders, J. J. Douth, A. M. Edwards, O. Ces and M. M. Stevens, *ACS Nano*, 2020, **14**, 17333–17353.
- 59 E. Beltrán-Gracia, A. López-Camacho, I. Higuera-Ciagara, J. B. Velázquez-Fernández and A. A. Vallejo-Cardona, *Cancer Nanotechnology*, 2019, **10**, 11.
- 60 V. V. S. N. L. Andra, S. V. N. Pammi, L. V. K. P. Bhatraju and L. K. Ruddaraju, *BioNanoScience*, 2022, **12**, 274–291.
- 61 S. Kansız and Y. M. Elçin, *Adv. Colloid Interface Sci.*, 2023, **317**, 102930.
- 62 J. Li, Z. Ge, K. Toh, X. Liu, A. Dirisala, W. Ke, P. Wen, H. Zhou, Z. Wang, S. Xiao, J. F. R. van Guyse, T. A. Tockary, J. Xie, D. Gonzalez-Carter, H. Kinoh, S. Uchida, Y. Anraku and K. Kataoka, *Adv. Mater.*, 2021, **33**, 2105254.
- 63 E. Rideau, R. Dimova, P. Schwille, F. R. Wurm and K. Landfester, *Chem. Soc. Rev.*, 2018, **47**, 8572–8610.
- 64 S. Iqbal, M. Blenner, A. Alexander-Bryant and J. Larsen, *Biomacromolecules*, 2020, **21**, 1327–1350.
- 65 T. Wang, J. Qin, J. Cheng, C. Li and J. Du, *Wiley Interdiscip. Rev.: Nanomed. Nanobiotechnol.*, 2022, **14**, e1822.
- 66 S. Matoori and J.-C. Leroux, *Mater. Horiz.*, 2020, **7**, 1297–1309.
- 67 M. Grit and D. J. A. Crommelin, *Chem. Phys. Lipids*, 1993, **64**, 3–18.
- 68 X. Wang, G. Liu, J. Hu, G. Zhang and S. Liu, *Angew. Chem., Int. Ed.*, 2014, **53**, 31038–31042.
- 69 H. Che, S. Cao and J. C. M. van Hest, *J. Am. Chem. Soc.*, 2018, **140**, 5356–5359.
- 70 Y. Zhu, S. Cao, M. Huo and J. C. M. van Hest, *Chem. Sci.*, 2023, **14**, 7411–7437.
- 71 G. Appendino, A. Minassi, N. Daddario, F. Bianchi and G. C. Tron, *Org. Lett.*, 2002, **4**, 3839–3841.

